Experimental Demonstration of Optical Guided-Wave Butler Matrices

John T. Gallo, *Member, IEEE* and Richard DeSalvo, *Member, IEEE*

***Abstract*—We report fully functional fiber-optic and integrated-optic Butler matrices, each with four input channels and four output channels. Simulated antenna excitation is modulated onto the four input optical channels to predict these devices' performance when employed with circular antenna arrays for angle-of-arrival applications. Heterodyne detection techniques are employed to recover the RF signal at the optical output of the matrices and for conversion to an intermediate frequency. An RF pilot tone is injected at the input to calibrate the system, and an active feedback loop maintains the proper phasing of the light channels.**

***Index Terms*— Direction of arrival estimation, heterodyning, integrated optoelectronics, optical fibers, optical phase-locked loops.**

I. Introduction

MODULATION of microwave signals onto an optical carrier enables broad-band microwave systems to be implemented using narrow-band coherent optical-processing techniques. Processing lengths scale to the optical wavelengths rather than those of the microwaves, resulting in a potential reduction of system size. Regrettably, greater phase sensitivity is incurred; a factor that is critical in many coherent optical systems. Multichannel systems suffer severe performance degradation without phase stability, prompting the use of active phase-control techniques.

Optical control of phase array antennas has long been a topic of research [1]. Several methods that have been recently reported include acoustically driven integrated optical circuits [2], fiber optics [3], [4], and bulk liquid-crystal devices [5]. The use of Butler matrices with antenna arrays for signal distribution and angle-of-arrival determination has been considered for many years [6]. Recent research has been directed toward photonic implementation of Butler matrices, both in bulk acousto-optic devices [7] and in guided-wave circuits [8], [9]. Difficulties with phase stability and fabrication tolerances have limited the number of channels available with guided-wave devices being reported to date. Phase-locked loops (PLL's) have been demonstrated [10] in fiber-fed phased-array antenna systems to overcome this problem.

We report an intermediary result of ongoing work on guided-wave Butler matrices for angle-of-arrival detection. Devices with only four channels are required for this application. Fiber-optic Butler matrix (FOBM) and integrated-optic Butler matrix (IOBM) 4×4 channel devices have been demonstrated. A computer-moderated active phase-control loop has allowed the implementation of a fiber-optic device composed entirely of commercially available components. A custom-built integrated-optic device also employs active phase control but provides better system performance. It is expected that the active phase-control method is adaptable to other coherent optical-processing systems, provided that the number of channels does not grow much beyond four.

Manuscript received December 4, 1996; revised April 28, 1997. This work was supported by S. Rodrigue and by Wright-Patterson Air Force Base.

J. T. Gallo was with the Harris Corporation, Government Communication Systems Division, Electro-Optics Center, Melbourne, FL 32902-9100 USA. He is now with Tracor Aerospace Electronics Systems, Inc., Melbourne, FL 32902-9100 USA.

R. DeSalvo is with the Harris Corporation, Goverment Communication Systems Division, Electro-Optics Center, Melbourne, FL 32902-9100 USA.

Publisher Item Identifier S 0018-9480(97)06014-6.

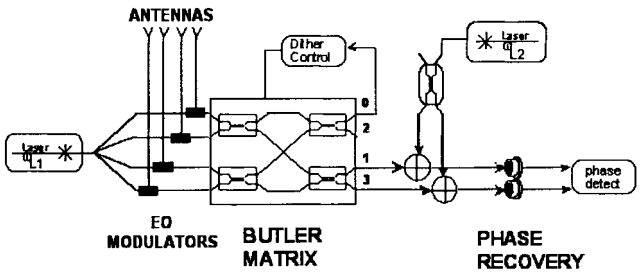

Fig. 1. Angle-of-arrival system topology.

II. Theory

The proposed system topology is shown in Fig. 1. A signal laser is used to feed four separate electro-optic phase modulators that are driven by the elements of an antenna array. This array is presumed circular in our application. The optical Butler matrix transforms the antenna signals, which are then mixed with a local oscillator (LO) laser and detected. Angle-of-arrival data is taken from a phase comparison of the detected signals.

A. Modulation Technique Selection

Initially, a double-sideband suppressed carrier (DSB-SC) technique [11] had been selected for modulating the microwaves signals onto the optical carrier. This technique allows the use of an optical amplifier directly after the modulator, while the sideband still enjoys a high signal-to-noise ratio without the carrier saturating the amplifier. As the Butler matrix system *evolved* and phase control became a concern, pure phase modulation appeared a more favorable solution. By retaining the optical carrier with the sidebands, the active phase-control system tracks the optical carriers to adjust the phase in the Butler matrix channels. The feedback theory is discussed in more detail later in this section.

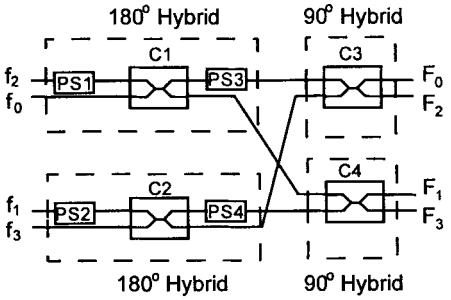

Fig. 2. A 4 × 4 Butler matrix implemented with 3-dB couplers (C) and phase shifters (PS) is shown. Bundling the phase shifters with the couplers allows comparison with matrices composed of 180° and 90° hybrids.

B. Optical Butler Matrix Theory

A Butler matrix is a passive phase-shifting network composed of directional couplers and phase shifters. Butler matrices perform a discrete Fourier transform of the M input channels on to the M output channels. Typically, 180° and 90° hybrids are used as the couplers [7] in microwave Butler matrices. A schematic of an optically implemented 4 × 4 Butler matrix is shown in Fig. 2. This system consists of 3-dB optical couplers and optical phase shifters connected and driven is such a way as to mimic microwave 180° and 90° hybrids.

Only the optical output of channels 1 and 3 (see Fig. 2) are required in angle-of-arrival (AOA) determination [7] from a four-element circular antenna array used in conjunction with a Butler matrix. These channels contain the fundamental (± 1) components of the Fourier transform. The generalized relationship for the output fields of an M-element Butler matrix is

$$F_k = \frac{1}{M}\sum_{m=0}^{M-1} f_m \exp(\mathrm{j}2\pi \mathrm{mk/M}) \tag{1}$$

where f_m is the mth input-channel field and F_k is the kth output-channel field.

The output fields of interest for the $M = 4$ channel device proposed in Fig. 2 are

$$F_1 = \frac{1}{4}(f_0 + f_1 e^{j\pi/2} + f_2 e^{j\pi} + f_3 e^{-j\pi/2}) \tag{2}$$

and

$$F_3 = \frac{1}{4}(f_0 + f_1 e^{-j\pi/2} + f_2 e^{j\pi} + f_3 e^{j\pi/2}). \tag{3}$$

The input optical fields are of the form $f_k = \sqrt{I_o}\exp(j[\omega_o t + \phi_k])$ where I_o is the light intensity, ω_o is the carrier's radial frequency and ϕ_k is the microwave signal that has been phase modulated onto the optical carriers.

Heterodyne reception is used to down-convert the signals from ports 1 and 3. As shown below, lower and upper sidebands contain the AOA data present at each of these ports and the unmodulated carrier signal has been stripped off by the Fourier transformation of the Butler matrix. The AOA may be measured directly as half the phase difference between ports 1 and 3 at either sideband. This requires either filtering to remove one sideband or setting the upper sideband beyond the detectors' frequency range.

C. Active Phase-Control Feedback

Several possible sources of phase error exist in our system including: 1) RF phase integrity of the antenna feed system; 2) amplitude balancing errors in the Butler-matrix components; 3) phase balance of the optical paths within the Butler matrix; 4) crosstalk terms at the output ports; and 5) separate optical LO paths before combination with the signal paths. Fortunately, the current work is not concerned with correcting phase-error problems in the RF signal (considered to be ideal) between the antennas and the electro-optic modulators. Only monitoring and correction of the optical phases are considered here.

Tracking of the phase relationships may be done by monitoring the unmodulated carrier signal at the output ports. Correction of phase errors requires active phase shifters on the optical channels. Our method of achieving proper phasing of the matrix is with a phase-dithering algorithm, whereby paired low-frequency signals are imposed on the input optical channels. The phase error is determined by monitoring the low-frequency output of the matrix and using the error signal to drive a phase shifter positioned to alter the relative phase between a pair of channels.

The feedback algorithm is based upon correcting the phase error between the two inputs to each 3-dB coupler simultaneously. In a 4 × 4 Butler matrix, four concurrent phase-control feedback loops are necessary. Dither tones were introduced to allow each feedback loop to discriminate its driving signal; hence, four dither tones are used. The number, P, of 3-dB coupler/phase-shifter pairs (dither tones) for an $M = 2^N$ channel Butler matrix is $P = N2^{N-1}$. This leads to rapid growth in required dither tones (i.e., when $M = 8$, $P = 12$) as the number of channels increase. The number of optical detectors required is $M/2$, which may become prohibitive.

The dither signals were modulated onto the carrier channels prior to being input to the Butler matrix. The output of the Butler matrix is detected, ac-coupled, and low-pass filtered to separate the low-frequency dither signals from the dc component and the RF signals. It should be noted that the two output ports used for the feedback loops are ports 0 and 3 *without mixing in the LO*.

The instantaneous phase error at the output port may be resolved by integrating the ac-coupled signal over each dither period. The ac-coupled signal is multiplied by cosine components of the dither frequencies, but only integrated over a single dither period. This allows a single detector to be used to monitor several dither frequencies. The error signals at any one frequency only relate to the phase error in that particular loop. The software loop driving the feedback was adjusted to provide phase accuracy of ± 1°.

III. Device Construction

The heterodyne recovery process requires that the signal and LO light have the same polarization at the detectors. Additionally, the signal channels must have the same polarization to assure proper mixing of the input channels through the Butler matrix. These considerations dictate the use of polarization maintaining (PM) or polarizing (PZ) components throughout the system. The optical wavelength was chosen as

1.32 microns because of the availability of extremely stable lasers with narrow linewidths and low-loss PM fiber at that wavelength.

A single laser is used to feed the four input channels. A Lightwave Electronics Model 2000 1.319-μm solid-state laser is fiber coupled to PM fiber then passed through a cascade of 2×2 fused PM-fiber couplers (made by the 3M Company) to create the four channels. Each channel then passes through a United Technologies phase modulator where the RF signal and low-frequency dither signal are modulated onto the carrier.

The fiber-optic matrix was made using standard 2×2 fused PM-fiber couplers and Canadian Instrumentation and Research LTD piezo-electric fiber stretchers as phase shifters. The integrated optical device was built to order by UTP. It has four Mach–Zehnder modulators that are biased to act as 3-dB couplers. Phase shifters have been placed in the circuit just as in the FOBM (according to Fig. 2).

The circular antenna designed to work with the guided-wave Butler matrices was not available for testing. This antenna was designed to operate from 20 MHz to 20 GHz, which was the design specification for the optical Butler matrices. In the absence of the antenna, a 4×4 RF Butler matrix composed of Merrimac 180° and 90° hybrids was built to feed the phase modulators. We chose to operate the device at 680 MHz, which provided the flattest response during RF testing even though the phase modulators had a maximum operating frequency of 1 GHz. The IOBM has a bandwidth slightly larger than 4 GHz but our test equipment limited our ability to exercise that bandwidth.

The RF feed electronics are shown in Fig. 3. One part of the RF signal was retarded using a Lorch electronic phase shifter and it was fed into one of the RF Butler matrix inputs while the unretarded signal was fed to the conjugate input. The remaining two RF inputs were not used. The four output ports of the RF Butler matrix were connected to the four phase modulators on the four optical channels of the guided-wave Butler matrix. A pilot tone at 750 MHz was split and injected along with the signal tone, albeit without any phase retarding, in order to monitor phase drift in the system output.

Feeding the optical phase modulators with RF signals whose phase relationships were created with an RF Butler matrix does not accurately emulate the operation of a circular antenna array. It does, however, allow the operation of the optical Butler matrix to be fully tested, which is the object of this paper. The input to the RF Butler matrix is Fourier transformed to the RF output that is fed to the optical phase modulators. These optical signals are then Fourier transformed by the optical Butler matrix, effectively retransforming the RF signal. The detected optical output should be an exact copy of the RF feed signal that was split and phase retarded but at an intermediate frequency (IF) defined by the LO laser-offset frequency.

Consider an RF field applied to the two inputs of the RF Butler matrix that is described by the equations

$$E_{\mathrm{RF1}}(t) = E_0 \cos(\omega_{\mathrm{m}} t)$$
$$E_{\mathrm{RF4}}(t) = E_0 \cos(\omega_{\mathrm{m}} t + \theta) \tag{4}$$

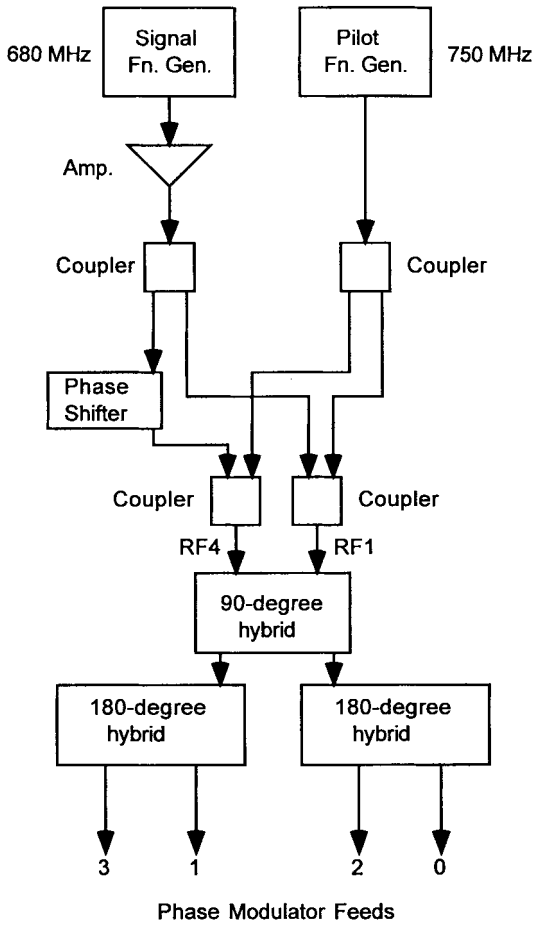

Fig. 3. The input feed electronics for generating the RF signals and pilot tones that drive the optical phase modulators is shown. The feed network is an RF Butler matrix (two of the four inputs are not shown) into which is fed an asymmetric RF signal and a symmetric pilot tone.

where E_0 is a constant, ω_m is the radial RF-signal frequency, and θ is the phase shift imparted by the electronic phase shifter. The signal applied to the optical phase modulators may be written as

$$\begin{aligned}
\phi_0(t) &= \beta[\sin(\omega_{\mathrm{m}} t + \theta) - \cos(\omega_{\mathrm{m}} t)] \\
\phi_1(t) &= \beta[\cos(\omega_{\mathrm{m}} t + \theta) - \sin(\omega_{\mathrm{m}} t)] \\
\phi_2(t) &= \beta[-\sin(\omega_{\mathrm{m}} t + \theta) + \cos(\omega_{\mathrm{m}} t)] = -\phi_0 \\
\phi_3(t) &= \beta[-\cos(\omega_{\mathrm{m}} t + \theta) + \sin(\omega_{\mathrm{m}} t)] = -\phi_1
\end{aligned} \tag{5}$$

where $\beta(\beta = \pi V/V_\pi)$ is the modulation index (assumed equal) of the phase modulators, V is the applied RF voltage, and V_π is the phase modulator's half-wave voltage. These applied signals have a different phase relationship than a four-element circular antenna array resulting in a measured phase difference at the output of θ instead of 2θ for a circular array.

These equations are substituted into (2) for the electric field at the output of F_1 (a similar analysis was used for F_3). The resultant field expression is

$$F_1 = \frac{\sqrt{I_o}}{4}\left(e^{j(\omega_o t + \phi_0)} + e^{j(\omega_o t + \phi_1 + \pi/2)} + e^{j(\omega_o t + \phi_2 + \pi)} + e^{j(\omega_o t + \phi_3 - \pi/2)}\right) \tag{6}$$

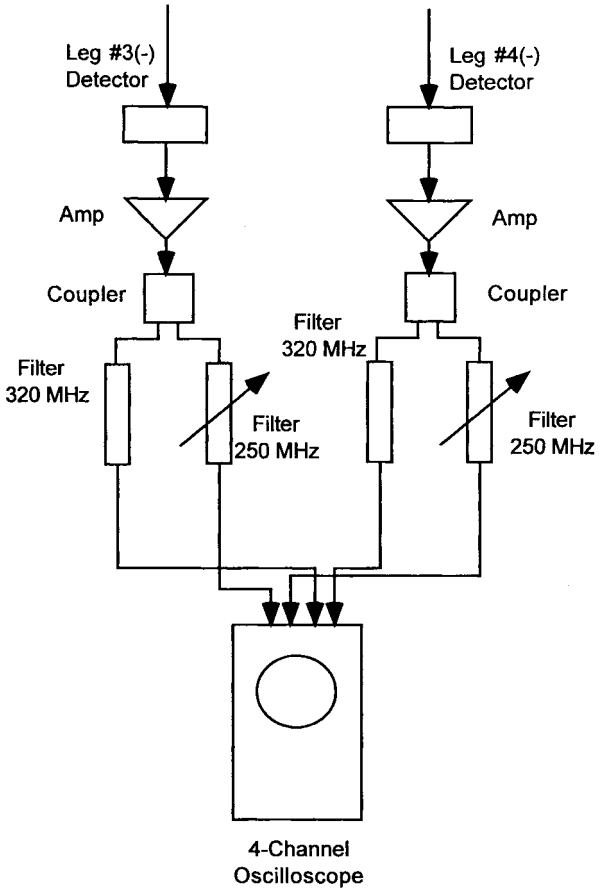

Fig. 4. The output electronics used in detecting and measuring the relative phases between the signal and pilot-tone output are shown.

which may be simplified using standard trigonometry and the relationships $\phi_2 = -\phi_0$ and $\phi_3 = -\phi_1$. The simplified expression is

$$F_1 = \frac{\sqrt{I_o}}{2} e^{j\omega_0 t}(-\sin\phi_1 + \mathrm{j}\sin\phi_0). \tag{7}$$

This signal is then mixed with light from the LO which may be written in the form $F_{\mathrm{LO}} = \sqrt{I_{\mathrm{LO}}}\exp(j[\omega_o + \omega_i]t)$ where ω_i is offset frequency between the signal laser and the LO. The detected signal power at *Port 1* may be written as the squared magnitude of the sum of these signals:

$$\text{Port } 1 = |F_1 + F_{\mathrm{LO}}|^2 = F_1F_1^* + F_1F_{\mathrm{LO}}^* + F_1^*F_{\mathrm{LO}} + F_{\mathrm{LO}}F_{\mathrm{LO}}^* \tag{8}$$

where the asterisks denote complex conjugation.

The detected electrical signals are found by substituting the equations for F_1 and F_{LO} into (8) and ignoring terms that are either dc or far above the detector's bandwidth (i.e., ignore $F_1F_1^* + F_{\mathrm{LO}}F_{\mathrm{LO}}^*$). The result is

$$\begin{aligned}\text{Port } 1 &\cong F_1F_{\mathrm{LO}}^* + F_1^*F_{\mathrm{LO}} \\ &\cong \frac{\sqrt{I_oI_{\mathrm{LO}}}}{2}[e^{-j\omega_1 t}(-\sin\phi_1 + \mathrm{j}\sin\phi_0) \\ &\quad + e^{j\omega_1 t}(-\sin\phi_1 - \mathrm{j}\sin\phi_0)] \\ &\cong \frac{2}{\sqrt{I_oI_{\mathrm{LO}}}}(\sin\phi_0\sin\omega_{\mathrm{i}}\mathrm{t} - \sin\phi_1\cos\omega_{\mathrm{i}}\mathrm{t}) \end{aligned} \tag{9}$$

TABLE I
RF BUTLER-MATRIX OUTPUT MEASURED AT THE ELECTRO-OPTIC (EO) PHASE MODULATORS. PARENTHETICAL ANGLES CORRESPOND TO IDEAL OPERATION OF THE RF BUTLER MATRIX

RF Input	Phase at EO Modulators			
	PM1	PM2	PM3	PM4
RF1	0°(0°)	256°(270°)	180°(180°)	69°(90°)
RF4	264°(270°)	−16°(0°)	84°(90°)	163°(180°)

	Amplitude at EO Modulators			
RF1	37.6 *mV*	28.8 *mV*	27.0 *mV*	43.0 *mV*
RF4	38.2 *mV*	28.2 *mV*	28.2 *mV*	41.2 *mV*

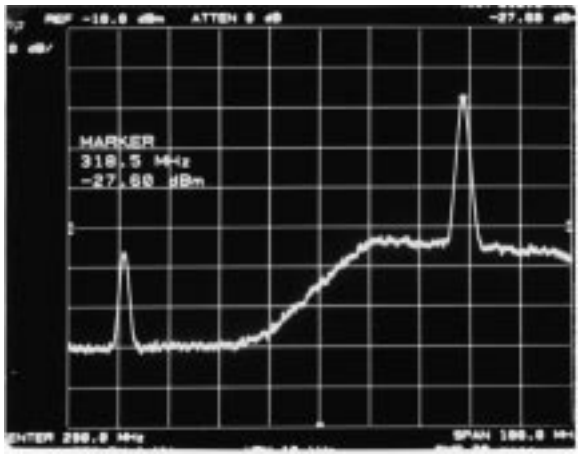

Fig. 5. Output spectrum of port 3 without filtering showing the pilot IF at 250 MHz and the signal IF at 320 MHz.

which may be further simplified using the trigonometric relationships

$$\begin{aligned}\sin(\alpha - \beta) &= \sin\alpha\cos\beta - \cos\alpha\sin\beta \\ \sin(\mathrm{z}\sin\alpha) &= 2\sum_{k=0}^{\infty} J_{2k+1}(z)\sin[(2\mathrm{k}+1)\alpha] \\ \sin(\mathrm{z}\cos\alpha) &= 2\sum_{k=0}^{\infty} (-1)^k J_{2k+1}(z)\cos[(2\mathrm{k}+1)\alpha] \\ \cos(\mathrm{z}\sin\alpha) &= J_o(z) + 2\sum_{k=1}^{\infty} J_{2k}(z)\cos 2\mathrm{k}\alpha \\ \cos(\mathrm{z}\cos\alpha) &= J_0(z) + 2\sum_{k=1}^{\infty} (-1)^k J_{2k}(z)\cos 2\mathrm{k}\alpha \end{aligned} \tag{10}$$

where J_n are nth-order Bessel functions of the first kind. After some tedious but straightforward algebra, the detected power in the fundamental signals at Port 1 may be written as

$$\begin{aligned}\text{Port } 1 = 2J_0(\beta)J_1(\beta)\sqrt{I_oI_{\mathrm{LO}}}(&\sin[\omega_{\mathrm{i}} - \omega_{\mathrm{m}}]\mathrm{t} \\ &+\cos[(\omega_{\mathrm{i}} + \omega_{\mathrm{m}})\mathrm{t} + \theta]) \end{aligned} \tag{11}$$

where the upper and lower sidebands are shown. Similarly, the power in the fundamental signals at Port 3 is

$$\begin{aligned}\text{Port } 3 = 2J_0(\beta)J_1(\beta)\sqrt{I_oI_{\mathrm{LO}}}(&\cos([\omega_{\mathrm{i}} - \omega_{\mathrm{m}}]\mathrm{t} - \theta) \\ &-\sin[\omega_{\mathrm{i}} + \omega_{\mathrm{m}}]\mathrm{t}). \end{aligned} \tag{12}$$

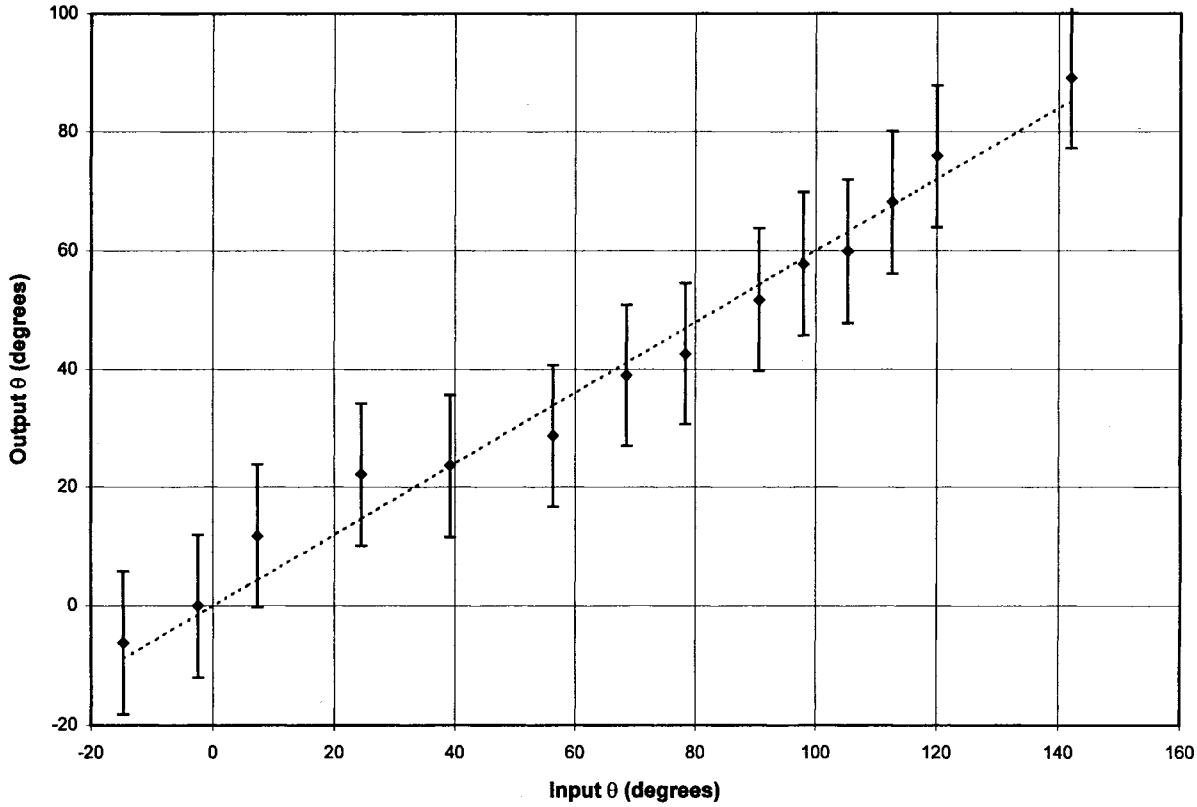

Fig. 6. Angle-of-arrival data taken with the fiber-optic Butler matrix. The signal phase has been corrected by subtracting the relative phase of the pilot tone. The pilot-tone phase fluctuated because of the relative phase drift between the signal laser and the LO laser. The slope of the recovered output phase data line is $C = 0.6$ and attributable to the nonideal Butler matrix used to feed the optical phase modulators.

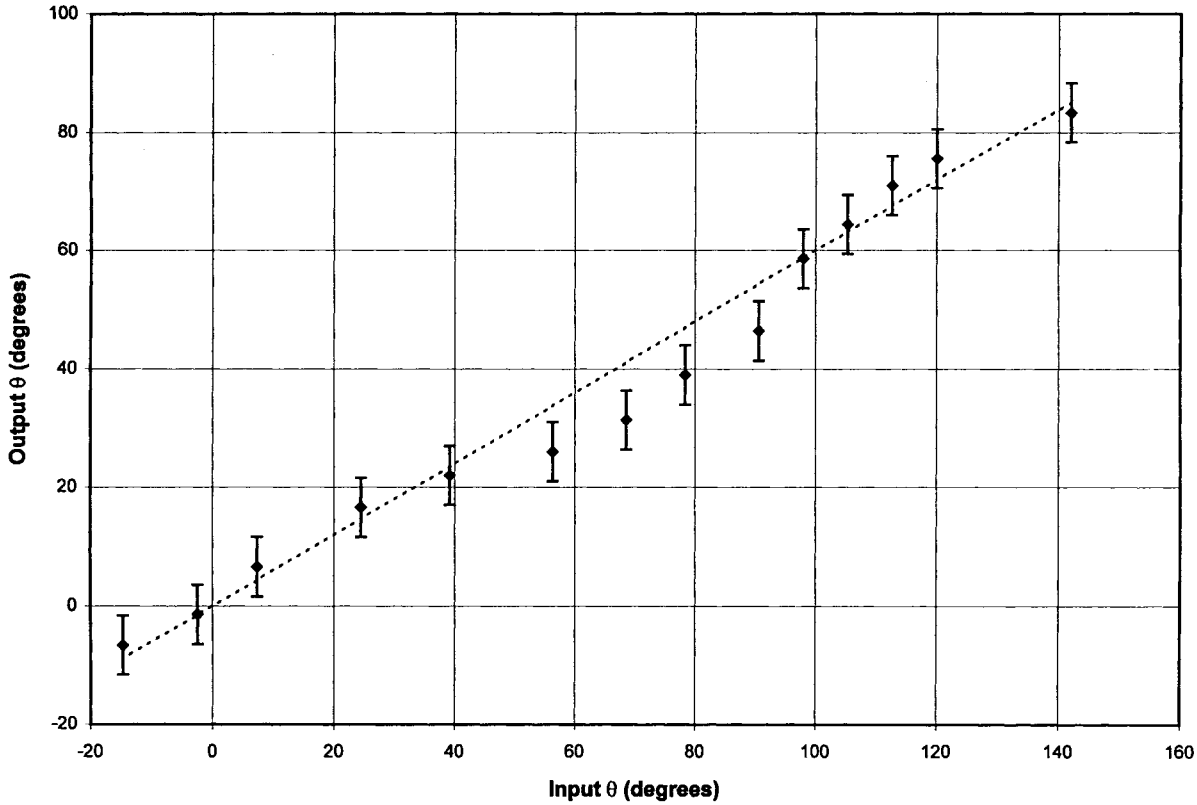

Fig. 7. Same as Fig. 6 with the integrated optical Butler matrix.

Note the RF phase shift θ occurs only in the upper sideband in (11) and only in the lower sideband in (12). Therefore, the lower sideband of the RF signal fed to input RF4 appears at output port 3 and the upper sideband at output port 1. Conversely, the lower sideband due to the input at RF1 appears at output port 1 and the upper sideband at output port 3. If we compare the phases of the upper sidebands or lower sidebands, their phase difference is θ.

The output electronics schematic is shown in Fig. 4. The output signals from ports 1 and 3 are amplified and split so that we may observe the relative phases of the RF signal and pilot tone separately. Filters are used to isolate the signal and pilot tones. The four output signals are observed on a four-channel oscilloscope and the relative phases of each pair recorded as a function of applied voltage to the electronic phase shifter.

IV. Experimental Data

The performance of the RF Butler matrix was not ideal. There was an amplitude imbalance across the four RF Butler-matrix outputs and they were not separated in phase by exactly 90°. Table I shows the RF signal phases and amplitudes measured at the electro-optic phase modulators due to input signals applied either to RF1 or RF4. The ideal RF Butler matrix should show the phases in parentheses and the amplitudes should all be equal. This data was taken at a frequency of 680 MHz, which came closest to the ideal case.

The LO laser was frequency offset from the signal laser by 1 GHz, resulting in lower sideband intermediate frequencies for the signal at 320 MHz and for the pilot tone at 250 MHz. These frequencies were chosen for compatibility with our limited test equipment and do not approach the limits of the device. Peaks of the lower sidebands at the pilot IF and signal IF are seen in the photograph of the output spectrum from port 3 without filtering (Fig. 5).

Nonideal operation resulted in the output phases of the optical signals not tracking the input electrical phase exactly. The output phase does linearly track with the input phase according to the equation

$$\theta_{\text{out}} = C\theta_{\text{in}} \tag{13}$$

where $C = 1$ for the ideal case. However, with the nonideal RF Butler-matrix input to the optical phase modulators, we no longer achieve a strict separation of the upper and lower sidebands between the output ports.

The RF1 and RF4 (see Fig. 3) ports were fed separately and the output tuned to detect the lower sidebands. Ideal operating of the Butler matrix should result in the lower sideband from RF1 appearing at *Port 3* only, and the upper sideband appearing at *Port 1* only (conversely for RF4 input). We experimentally measured lower sidebands at both output ports from RF1. The value of C is reduced in this case. For the sample data sets in Figs. 6 (FOBM) and 7 (IOBM), the slopes of the fitted lines are $C = 0.6$, which is constant both for the FOBM and IOBM supporting the hypothesis that this effect is solely due to the nonideal RF Butler matrix.

The drift of the pilot-tone phase was measured to be 0.14 rad/min at room temperature for the IOBM and roughly twice that for the FOBM. No measurements were conducted to test environmental effects on the drift. A fixed electronic phase was input to the device and measurement of the output phase made over 1 h. The detected signal phase drifted $\pm$ 5° over a period of 20 min for the IOBM and $\pm$ 12° for the FOBM. This drift is reflected in the error bars in Figs. 6 and 7.

V. Conclusion

Although the FOBM operated well in the laboratory, the exposed fiber made the system very sensitive to environmental changes. The IOBM has slightly better environmental stability but still suffers from the fiber network that led from the signal laser, through the 1×4 splitters and phase modulators before entering the IOBM. A bulky housing was manufactured to contain the system, which minimized the effects of environmental changes at the expense of system size and weight. The next generation device will include the 1×4 splitter and phase modulators on the same substrate as the 4×4 integrated-optical circuit implementation of the Butler matrix. This layout is expected to drastically reduce the environmental sensitivity and system size.

References

[1] A. Kumar, *Antenna Design with Fiber Optics.* Norwood, MA: Artech House, 1996, pp. 91–192.
[2] M. N. Armenise, V. M. N. Passaro, and G. Noviello, "Lithium niobate guided-wave beam former for steering phased-array antennas," *Appl. Opt.*, vol. 33, no. 26, pp. 6194–6209, Sept. 1994.
[3] K. E. Alameh, R. A. Minasian, and N. Fourikis, "High capacity optical interconnects for phases array beamformers," *J. Lightwave Technol.*, vol. 13, no. 6, pp. 1116–1120, June 1995.
[4] J. B. Georges and K. Y. Lau, "Broadband microwave fiber-optic links with RF phase control for phased-array antennas," *IEEE Photon. Technol. Lett.*, vol. 5, pp. 1344–1346, Nov. 1993.
[5] N. A. Riza, "A compact high-performance optical control system for phased array radars," *IEEE Photon. Technol. Lett.*, vol. 4, pp. 1072–1075, Sept. 1992.
[6] J. Butler and R. Lowe, "Beam-forming matrix simplifies design of electronically scanned antennas," *Electron. Design*, pp. 170–173, Apr. 1961.
[7] J. P. Y. Lee, "Two-dimensional acousto-optic processor using a circular antenna array with a Butler matrix," *Opt. Eng.*, vol. 31, no. 9, pp. 1999–2011, Sept. 1992.
[8] M. R. Surette, D. R. Hjelme, and A. R. Mickelson, "An optically driven phased array antenna utilizing heterodyne techniques," *J. Lightwave Technol.*, vol. 11, no. 9, pp. 1500–1509, Sept. 1993.
[9] W. Charczenko, M. Surette, P. Matthews, H. Koltz, and A. R. Mickelson, "Integrated optical Butler matrix for beam forming in phased array elements," *Proc. SPIE–Opt. Signal Processing for Phased-Array Antennas II*, pp. 196–206, 1990.
[10] W. M. Neubert, K. H. Kudielka, W. R. Leeb, and A. L. Scholtz, "Experimental demonstration of an optical phased array antenna for laser space communications," *Appl. Opt.*, vol. 33, no. 18, pp. 3820–3830, June 1994.
[11] R. Montgomery and R. DeSalvo, "A novel technique for double sideband suppressed carrier modulation of optical fields," *IEEE Photon. Technol. Lett.*, vol. 7, pp. 434–436, Apr. 1995.

John T. Gallo (S'86–M'91) received the M.S.E.E. and Ph.D. degrees in electrical engineering from the Georgia Institute of Technology, Atlanta, GA, in 1991.

Following graduation, he spend one year as an Invited Research Fellow at Osaka University, developing polymer waveguide materials and applications. From 1993 to 1994, he was with the Optoelectronic Computing System Center, University of Colorado at Boulder, developing liquid crystal waveguide components. From 1995 to 1997, he was with Harris Corporation's Electro-Optics Center engaged in research and development of guide-wave components for phased-array antenna systems. He is currently Principle Engineer with Tracor Aerospace Electronic Systems, Inc., Melbourne, FL, working on microwave fiber optic systems.

Dr. Gallo is a member of IEEE Lasers and Electro-Optics Society and IEEE Microwave Theory and Techniques Society.

Richard DeSalvo (S'89–M'90) received the B.S. degree in physics from Jacksonville University, Jacksonville, FL, in 1988, and the Ph.D. degree in physics from the University of Central Florida, Center of Research in Electro-Optics and Lasers, Orlando, FL, in 1993.

He is currently a Staff Engineer at Harris Corporation Government Communication Systems Division, Melbourne, FL, performing research and development in optical communication systems. His work includes broad-band analog coherent fiber-optic links, intersatellite optical communication links, hybrid analog/digital wavelength-division multiplexed links, and erbium-doped fiber amplifier applications in analog optical links.

Dr. DeSalvo is a member of the Optical Society of America.